

MATHEMATICAL ANALYSES OF EFFECT OF HYDROGEN ON FATIGUE BEHAVIOUR OF FOUR STAINLESS STEELS

Tsvetelina LAZAROVA, Rozina YORDANOVA, Donka ANGELOVA

University of Chemical Technology and Metallurgy, Sofia, Bulgaria, EU, tsveti26@yahoo.com

Abstract

Fatigue in stainless steel-candidates for hydrogen storage and infrastructure is described mathematically at different loading conditions. The investigated steels are: EN10095 1.4301, EN10095 1.4401, EN10095 1.4404 and EN10095 1.4002.

All the tests are carried out under tension-compression fatigue at different loads and a stress ratio $R = -1$. Specimens are machined in hour-glass shape with artificial hole from which initial cracks start their propagation. For finding the effect of hydrogen on fatigue behaviour of investigated steels, the specimens are divided into two groups: of hydrogen charged and uncharged ones.

The obtained fatigue data of each steel are presented in plots "Crack length - Number of cycles" and "Fatigue crack growth rate - Crack length". A mathematical model is found for the data in the presentation "Fatigue crack growth rate - Crack length". The model consists of double-parabolic-linear-curve for all steels, which makes it possible to prognosticate their fatigue behaviour under different loading conditions. The adequacy of the presented model is checked and proved by comparison between experimental fatigue lifetimes and those calculated by the model.

Keywords: Fatigue, hydrogen fatigue, stainless steel, short fatigue crack, short fatigue crack growth rate

1. INTRODUCTION

The materials used for the components of fuel cell vehicles (FCVs), and stationary fuel cell (SFC) systems, equipment for hydrogen stations, hydrogen pipelines and transport systems are directly exposed to high-pressure hydrogen. Deep research on such materials is done in Kyushu University, Japan, [1, 2], where Murakami and team investigated the effect of hydrogen on fatigue crack growth behaviour, including the measurement of the hydrogen content in microstructure.

The aim of this work is to investigate fatigue behaviour of steels used for hydrogen materials, under different conditions. This was accomplished by performing the following steps:

- Using the obtained by Murakami fatigue data we present them in plots "Crack length - Number of cycles" and "Fatigue crack growth rate - Crack length";
- Modelling of data by proposing a system of parabolic-linear functions;
- Checking of the adequacy of the proposed model;
- Comparison and analysing of the results.

To clarify the influence of the hydrogen charging the results of the hydrogen charged (H-charged) and uncharged (Uncharged) specimens were compared.

2. MATERIAL AND EXPERIMENTAL WORK CONDUCTED BY MURAKAMI

In this work data about fatigue crack propagation in construction steels, published by Murakami, were used.

2.1 Materials and specimens

The materials used are SUS304 (EN10095 1.4301), SUS316 (EN10095 1.4401), SUS316L (EN10095 1.4404) and SUS405 (EN10095 1.4002) [1, 2]. **Table 1** shows the chemical compositions and the Vickers hardness of these materials.

Table 1 Chemical composition of the stainless steels and their Vickers hardness

	Vickers hardness	Chemical composition (wt. %)									
	HV	C	Si	Mn	P	S	Ni	Cr	Mo	Cu	Al
SUS304	176	0.06	0.36	1.09	0.030	0.02	8.19	18.7	-	-	-
SUS316	161	0.05	0.27	1.31	0.03	0.03	10.2	17.01	-	2.04	-
SUS316L	157	0.019	0.78	1.40	0.037	0.01	12.08	17.0	2.04	-	2.6
SUS405	159	0.04	0.37	0.38	0.02	0.01	0.21	13.2	-	-	0.26

The specimens were machined in hour glass shape (**Fig. 1a**) with artificial hole (diameter $d = 100 \mu\text{m}$ and depth $h = 100 \mu\text{m}$, as shown in **Fig. 1b**). All specimens were polished mechanically to removing all rough surfaces with #2000 emery paper. After that the specimen surface was finished by buffing using colloidal SiO_2 (0.04 μm) solution.

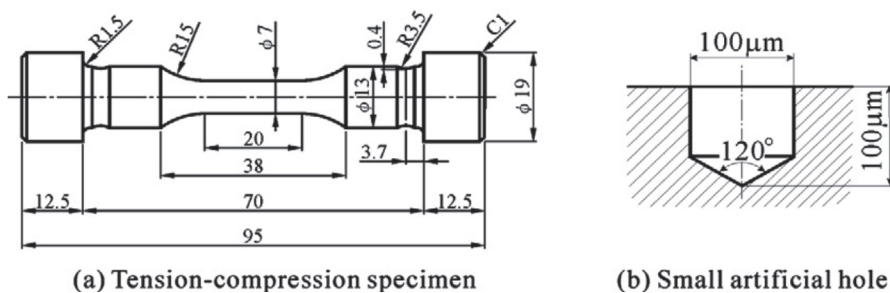


Fig. 1 Geometry and dimensions of fatigue test specimens, in mm

2.2 Grouping of used materials

All specimens from steel type SUS304 are marked as Group A, the specimens made from type 316 - as Group B, from type 316L - Group C and from type 405 - Group D. The four groups are divided into two subgroups and marked with a subscript "1" or "2" for hydrogen-charged and hydrogen-uncharged specimens respectively. In **Table 2** is shown the distribution of groups.

Table 2 Grouping of used stainless steels

Stainless steel	Experimental conditions	Group
SUS304 (Austenitic)	tension-compression, $\sigma_a = 280 \text{ MPa}$, $f = 1.2 \text{ Hz}$	Group A_1 - Hydrogen-charged
		Group A_2 - Uncharged
SUS316 (Austenitic)	tension-compression, $\sigma_a = 260 \text{ MPa}$, $f = 1.2 \text{ Hz}$	Group B_1 - Hydrogen-charged
		Group B_2 - Uncharged
SUS316L (Austenitic)	tension-compression, $\sigma_a = 260 \text{ MPa}$, $f = 5 \text{ Hz}$	Group C_1 - Hydrogen-charged
		Group C_2 - Uncharged
SUS405 (Ferritic)	tension-compression, $\sigma_a = 270 \text{ MPa}$, $f = 15 \text{ Hz}$	Group D_1 - Hydrogen-charged
		Group D_2 - Uncharged

2.3 Hydrogen charging

Hydrogen was charged into the specimens of stainless steels SUS 304, SUS 405, SUS316 and SUS316L by cathodic charging. The solution used for the cathodic charging was a dilute sulphuric acid (PH = 3.5) and the current density was $i = 27 \text{ A/m}^2$. Hydrogen charging conditions for fatigue test specimens are shown in **Table 3**, [1, 2].

Table 3 Hydrogen charging conditions

	Charging method	Charging time (h)	Temperature of solution (°C)	Hydrogen content of uncharged specimen (ppm)	Hydrogen content of cross section of hydrogen-charged specimen HC
SUS304	Cathodic	672	50	2.2	3.7 ppm (14 h after HC)
SUS316	Cathodic	672	50	3.4	5.5 ppm (102 h after HC)
SUS316L	Cathodic	672	50	2.7	4.3 ppm (81 h after HC)
SUS405	Cathodic	336	50	0.1	2.1 ppm (27 h after HC)

2.4 Fatigue testing

The surface short - crack propagation on the hour-glass specimens was monitored by acetate-foil replica technique during a fixed interval of fatigue cycles and observed on the replicas by an optical microscope for measuring registered surface crack lengths. Fatigue tests of the H-charged and Uncharged specimens were carried out at room temperature in laboratory air. Tension-compression fatigue tests were carried out at stress ratio $R = -1$ and at a different testing frequency (f) and different stress ranges (σ_a) shown below.

2.5 Experimental procedure

The effect of hydrogen on fatigue crack behaviour of stainless steels was investigated by Murakami at following sequence:

- The surface short-crack propagation on hour-glass specimens was monitored by acetate-foil replica technique during a fixed interval of fatigue cycles and observed on the replicas by an optical microscope for measuring registered surface crack lengths [1,2]
- Data obtained from tension compression fatigue test - crack lengths a , (μm) and the corresponding numbers of cycles N (cycles) - are plotted as "Crack length - Numbers of cycles," are shown in **Fig. 2**.

3. NEWLY PROPOSED MATHEMATICAL DESCRIPTION OF THE PROCESS

Crack growth rate da/dN [$\mu\text{m}/\text{cycle}$] is determined as a ratio of divided differences between two consecutive values of a [μm] and N [cycles]. To describe the fatigue behaviour during the different stages of crack growth is proposed the following mathematical model in Eq. 1 in log-log scale, [3-8].

There are three stages of fatigue crack propagation. During the first stage called Stage of short fatigue crack growth (SFC) fatigue cracks initiate and propagate as shear cracks - MODE II. Entering into the second stage known as Stage of physically small fatigue crack growth (PhSFC) the shear fatigue cracks change into tensile cracks - MODE I. During these two stages fatigue cracks are strongly influenced by different elements of metal microstructure, and their propagation can be described by parabolic functions. The third stage, Stage of long fatigue crack growth (LFC), shows that metal microstructure does not influence fatigue crack growth and fatigue crack propagates with increasing rate up to the complete failure of specimen. The modelling of this stage uses linear function.

$$\mathbf{M(a):} \begin{cases} \text{SFC: } \left(\frac{da}{dN} \right)_{sh} = D_1 a^2 + D_2 a + D_3; a \in [a_0, d_1] \\ \text{PhSFC: } \left(\frac{da}{dN} \right)_{phs} = D_4 a^2 + D_5 a + D_6; a \in [d_1, d_2] \\ \text{LCF: } \left(\frac{da}{dN} \right)_l = D_7 a^{D_8}; a \geq d_2 \end{cases} \quad (1)$$

where d_1 is the border between the stages.SFC, PhSFC and d_2 - between the stages PhSFC, LFC;

a_0 [μm] is the initial crack length and a_f [μm] - the final crack length at failure. The values of all material constants - coefficients D_i - in equations of (1) are determined by using the least - square method.

4. RESULTS AND DISCUSSION

Obtained fatigue data are presented in plots “Crack length - Number of cycles” for charged and uncharged specimens and shown in **Fig 2 a, b, c, d**, respectively for group A,B,C,D:

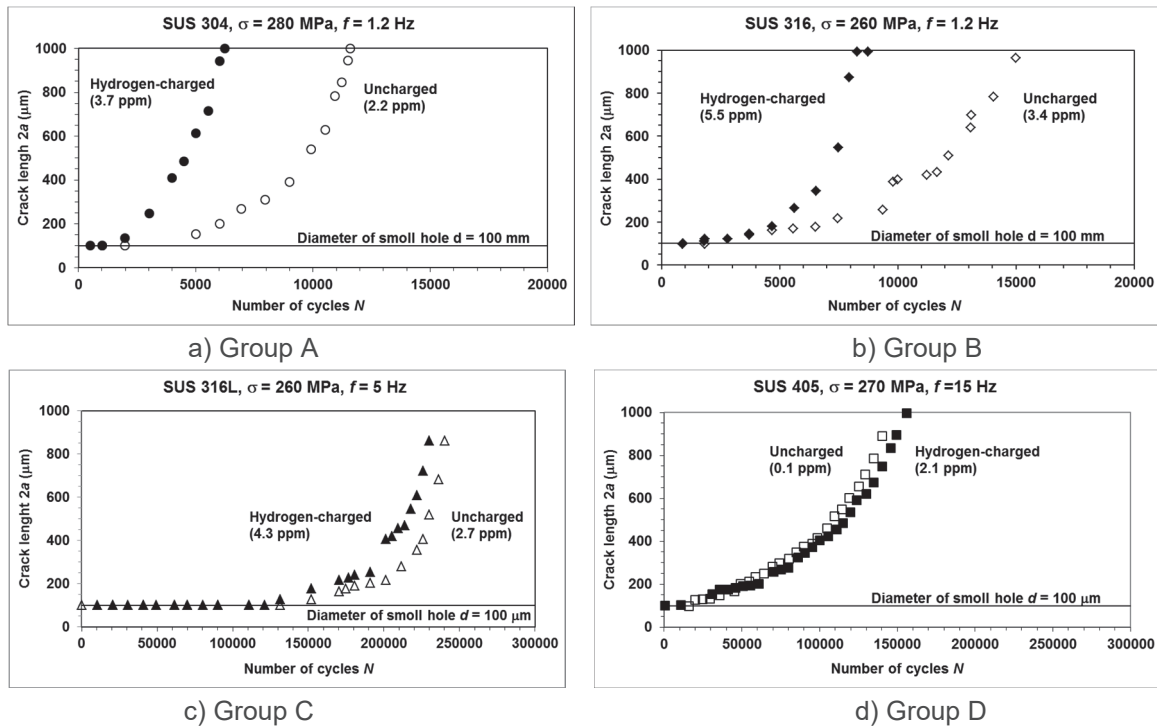


Fig. 2 Crack growth length, $2a$ versus number of cycles, N . Hydrogen content of specimen was measured immediately after fatigue test

Fig. 2 shows the fatigue crack growth curves starting from a hole in the uncharged and hydrogen-charged specimens of the mentioned four groups. The hydrogen content values in this figure were measured immediately after the fatigue test by thermal desorption spectrometry (TDS). For both SUS304 and SUS316, hydrogen charging led to a marked increase in fatigue crack growth rate, **Fig.3 a,b**. However for both SUS316L and SUS405 there was little if any effect of hydrogen charging on fatigue crack growth, **Fig.3 c,d**.

In this work we propose a modelling of short fatigue crack growth rate using equation (1), [6]. The values of all coefficients D_i calculated by the model for the different groups of specimens are shown in **Table 4**.

Mechanical and microstructural characteristics, crack length, fatigue lifetimes calculated by the model and obtained experimentally and corresponding errors are shown in **Table 5**.

Using data from **Table 4** and estimating equations (2, 3) we present the obtained results in **Table 5**. The proposed model is supported by the comparison of the fatigue lifetime predicted by Equation (3), $N_{f,mod}$, and the actual fatigue lifetime, $N_{f,exp}$ and results are shown in last column of **Table 5**.

$$N_{f,mod} = N_0 + \int_{a_0}^{d_1} \frac{1}{(D_1 a^2 + D_2 a + D_3)} da + \int_{d_1}^{d_2} \frac{1}{(D_4 a^2 + D_5 a + D_6)} da + \int_{d_2}^{a_f} \frac{1}{D_7 \cdot a^{D_8}} da, \quad (2)$$

where N_0 is the number of cycles for crack initiation.

$$S = 100(N_{f, \text{exp}} - N_{f, \text{mod}}) / N_{f, \text{exp}} \quad (3)$$

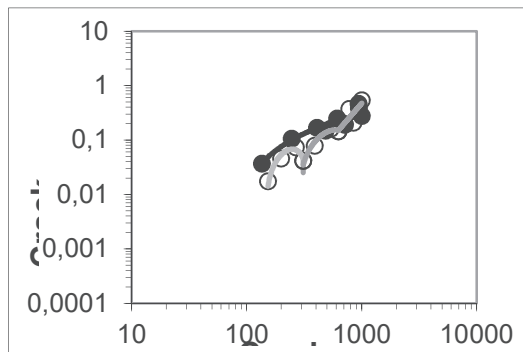
Comparison between models of data for H - Charged and Uncharged specimens is shown in Fig.3:(a) Group A , (b) Group B, (c) Group C and (d) Group D.

Table 4 Coefficients D_i for different stress ranges and for the different groups of specimens

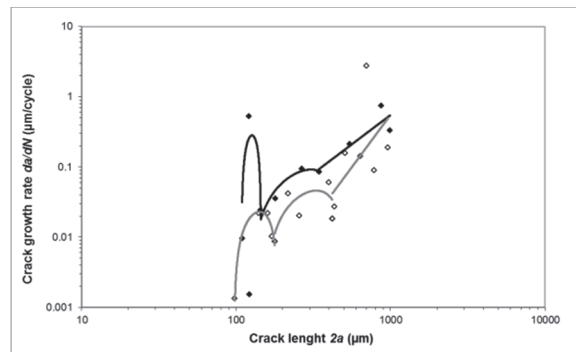
Group	I stage (SFC)			II stage (PhSFC)			III stage (LFC)	
	D_1	D_2	D_3	D_4	D_5	D_6	D_7	D_8
A_1				-5.42×10^{-7}	7.57×10^{-4}	-5.43×10^{-2}	1.90×10^{-6}	1.763
A_2	-5.85×10^{-6}	2.91×10^{-3}	-2.95×10^{-1}	-1.47×10^{-6}	1.75×10^{-3}	-3.66×10^{-1}	2.27×10^{-8}	2.439
B_1	-8.34×10^{-4}	21.16×10^{-2}	-1.31×10^{-2}	-2.84×10^{-6}	1.74×10^{-3}	-17.38×10^{-2}	5.65×10^{-6}	1.663
B_2	-1.16×10^{-5}	32.78×10^{-4}	-20.91×10^{-2}	-1.49×10^{-6}	9.88×10^{-4}	-11.72×10^{-2}	6.50×10^{-14}	2.977
C_1	-2.15×10^{-7}	7.92×10^{-5}	-4.61×10^{-3}	-6.83×10^{-7}	50.77×10^{-5}	-83.46×10^{-3}	1.21×10^{-9}	2.531
C_2	-46.48×10^{-6}	10.38×10^{-3}	-56.14×10^{-2}	-1.39×10^{-7}	82.08×10^{-6}	-7.05×10^{-3}	2.79×10^{-7}	1.635
D_1	-11.44×10^{-7}	34.61×10^{-5}	-23.28×10^{-3}	-11.29×10^{-7}	20.46×10^{-8}	-12.43×10^{-3}	1.43×10^{-6}	1.372
D_2	-46.48×10^{-6}	10.37×10^{-3}	-56.14×10^{-2}	-1.39×10^{-7}	82.08×10^{-6}	-7.05×10^{-3}	2.79×10^{-6}	1.635

Table 5 Mechanical, microstructural characteristics, fatigue lifetimes and the corresponding errors S

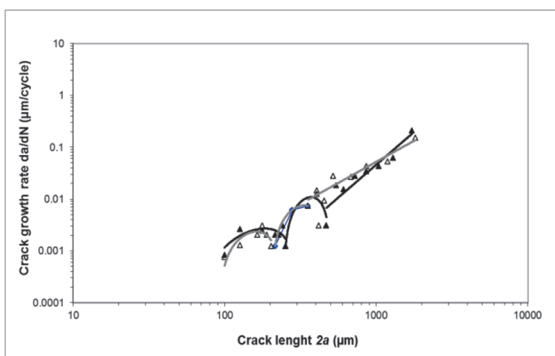
Group	σ_a (MPa)	f (Hz)	a_0 (μm)	N_0 (cycles)	a_f (μm)	d_1 (μm)	d_2 (μm)	$N_{f, \text{mod}}$ (cycles)	$N_{f, \text{exp}}$ (cycles)	S (%)
A_1	280	1.2	100	510	1000	485	714	7439	6230	19,4
A_2	280	1.2	100	1021	1000	310,6	629,8	11257	11592	-2,9
B_1	260	1.2	100	1818	1000	144.5	345	8368	8750	-4.0
B_2	260	1.2	100	1838	962	178	420	16003	15000	6.6
C_1	260	5	100	10274	1722	253	468.4	250273	240411	4.2
C_2	260	5	100	20548	1810	202.5	354.4	243345	250385	-2.9
D_1	270	15	100	673	1000	176	275	164059	156153	11.0
D_2	270	15	100	15781	889	130.7	388.8	142645	140417	1.6



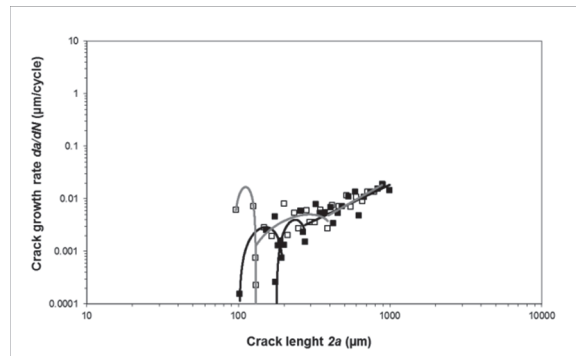
a) Group A



b) Group B



c) Group C



d) Group D

Fig. 3 Models for charged and uncharged specimens

Steels SUS 304, SUS 316, **Fig 3a** and **b**, show a big difference between behaviour of H - charged and Uncharged specimens, higher crack growth rates for the charged specimens. On the contrary, steels as SUS 405 and SUS 316L Fig c and d, show similar, and lower in some stages, crack growth rates, and only slightly shorter fatigue lifetimes.

CONCLUSIONS

For each steel obtained fatigue data are presented in plots "Crack length - Number of cycles" and "Fatigue crack growth rate - Crack length". Mathematical modelling was done and showed (qualitatively) the same double-parabolic-linear-curve presentation for all steels investigated in this work, which makes possible the prognostication of fatigue behaviour of different steels under different fatigue loading. The adequacy of presented models is checked and proved by comparison of experimental fatigue lifetimes and those calculated by the models.

Results for Steels SUS 304 and SUS 316 show a big difference between behaviour of H - charged and Uncharged specimens, shorter major fatigue crack lengths at fracture, higher crack growth rates for the charged specimens. On the contrary, steels as SUS 405 and SUS 316L show similar, and lower in some stages, crack growth rates, and only slightly shorter fatigue lifetimes and final (at fracture) crack lengths, which makes them good candidates for hydrogen storage and infrastructure applications.

ACKNOWLEDGEMENTS

This paper has been produced with the financial assistance of the European Social Fund, projects number BG051PO001-3.3.06-0014 and BG051PO001-3.3.06-0038.

The authors are responsible for the content of this material, and under no circumstances can be considered as an official position of the European Union and the Ministry of Education and Science of Bulgaria.

REFERENCES

- [1] MURAKAMI, Y. The effect of hydrogen on fatigue properties of metals used for fuel cell system. *Int. J. Fracture*, 138, 1-4, 2006, 167-195.
- [2] MURAKAMI, Y., MATSUOKA, S. Effect of hydrogen on fatigue crack growth of metals. *Eng. Fracture Mechanics*, 77, 2010, 1926-1940.
- [3] YORDANOVA, R. *Modeling of fracture process in a low-carbon 09Mn2 steel on the bases of short fatigue crack growth experiments. Comparative analyses on the fatigue behaviour of other steels.* Sofia, Bulgaria: University of Chemical Technology and Metallurgy, PhD Thesis, 2003. 265 p.
- [4] ANGELOVA, D., AKID, R. A. Note on Modelling Short Fatigue Crack Growth Behaviour. *Fatigue & Fracture of Eng. Mater. & Structures*, 21, 1998, 771-779.
- [5] YORDANOVA, R. On Modern fatigue approach included investigations of short fatigue cracks. In: Conf. Proc. Vol. II, *Tech. Nat. Sci.*, Plovdiv, Bulgaria: IMEON, 2007, 32-38.
- [6] YORDANOVA, R. Fatigue modeling based on Short Fatigue Crack Data, *10 Int. conference on metallurgy*, 28. - 31. 5. 2007. Varna, Bulgaria, [CD-ROM], Published by: Union of Bulgarian Metallurgists, 2007
- [7] ANGELOVA, D., YORDANOVA, R. Modelling of Fatigue in Some Steels and Non-Ferrous Alloys. In: 17th Europ. Conf. on Fracture "Multilevel Approach to Fracture of Materials, Components and Structures (ECF170)", Brno, 2008, Czech Republic, Congress e-Book, 819-826.
- [8] YORDANOVA, R., DAVIDKOV, A., MOYNOV, S., SAVOV, G. Modeling the behavior of the Fatigue crack. Methodology for Specifying the Model Functions. *J. of the UCTM*, 38, 4, 2003, 1197-1204.